Multiple Substitution Effects and Three-Dimensional Nonlinear Free-Energy Relationships in the Electrochemical Reduction of the *N,N′*-Dibenzyl Viologen and the 4-Benzoyl-*N*-benzylpyridinium Cation

Nicholas Leventis,*,† Mary Ann B. Meador,*,† Guohui Zhang,‡ Amala Dass,‡ and Chariklia Sotiriou-Leventis*,‡

Materials Division, NASA Glenn Research Center, 21000 Brookpark Road, Cleveland, Ohio 44135, and Department of Chemistry, University of Missouri-Rolla, Rolla, Missouri 65409

*Received: January 28, 2004; In Final Form: May 7, 2004*

The simultaneous effect of two substituents on the redox potentials, $E_{1/2}$'s, of *N,N′*-di(*p*-substituted benzyl)-viologens (**1-X,Y**) and of 4-(*p*-substituted benzoyl)-*N*-(*p*-substituted benzyl) pyridinium cations (**2-X,Y**), was investigated in terms of the substituent constants, σ_{p-X} and σ_{p-Y}. Systems **1-X,Y** and **2-X,Y** were chosen because they both undergo successive outer sphere one electron (1-e) reductions, and therefore there is no ambiguity regarding the mechanism or the rate-determining step. Substituents (X and Y) were chosen among the −NO₂, −Br, and −OCH₃ groups in six different combinations for **1-X,Y**'s and nine different ones for **2-X,Y**'s. Response surfaces are essentially three-dimensional Hammett plots. Statistical analysis according to a quadratic model derived from the Taylor series expansion of the general extrathermodynamic relationship $E_{1/2} = F(\sigma_{p-X}, \sigma_{p-Y})$ that describes the dependence of $E_{1/2}$'s on the substituent constants shows that the substitution effect is not additive. Quite strong nonlinear terms appear when substituents can interact through resonance with a site involved in the electron-transfer process. This, for example, is the case for the second -e reduction of **2-X,Y**'s. Other significant nonlinear effects are attributed to stereoelectronic effects in combination with the high polarizability of π-electrons. Our results have important implications on our ability to predict the effect of tuning of the redox potential of redox-active species through substitution.

Introduction

Curvature in Hammett "linear" free-energy (HLFE) relationships is associated traditionally with the reaction mechanism. Thus, curving up is usually attributed to a radical change in the mechanism (e.g., from S_N1 to S_N2), while curving down is usually attributed to a change in the rate-determining step within the same mechanism.[1] Nevertheless, even in well-established classes of reactions, as for example in certain cases of ester hydrolysis, nonlinearities of the second kind (curving down) may not be related to changes in the reaction mechanism, but rather to an increasing resonance stabilization of the ground state as substituents progressively become more electron-donating.[2] To account for such effects and restore linearity, HLFE relationships have been modified by introducing: (a) new sets of substituent constants (for example, refer to σ^+ and σ^-); and (b) different kind of plots (refer to the Brown and Okamoto or the Yukawa and Tsuno approaches).[3] Although the subject of nonlinear and nonadditive substitution effects has received past[4] and recent attention,[5] it has not been studied extensively from a fundamental, non-curve-fitting, perspective. In this context, usually nonadditive substitution effects are treated from an interactive viewpoint, without consideration of the possibility for nonlinear correlations within a single substitution pattern; treatments according to the More O'Ferrall equation,[6] which includes a square nonlinear term, are rather rare.

Curvature in Hammett relationships because of multisubstitution effects on electrochemical reactions has not received much

* To whom correspondence should be addressed. E-mail: Nicholas.Leventis@nasa.gov; Maryann.Meador@nasa.gov; cslevent@umr.edu.
† NASA Glenn Research Center.
‡ University of Missouri-Rolla.

systematic attention either. Multiple substitution has been proposed as a means for fine-tuning redox potentials,[7,8] and the possibility for "interdependence" between the relative effects of the different substituents has been mentioned.[8,9] In our opinion, on the other hand, outer sphere one-electron (1-e) transfer reactions ought to be ideal platforms for studying experimentally nonlinear free-energy effects, because they offer the advantage of one-step reactions with no mechanistic ambiguity, and thus all nonlinear substitution effects will have to be attributed solely to stereoelectronic interactions of the reaction site with the substituents. In this context, here we consider two systems, one symmetric (dibenzyl viologen, **1-X,Y**) and one unsymmetric (the 4-benzoyl-*N*-benzylpyridinium cation, **2-X,Y**), and we investigated the effect of multiple substitution over the two-dimensional domain defined by −X and −Y.

1-X,Y

2-X,Y
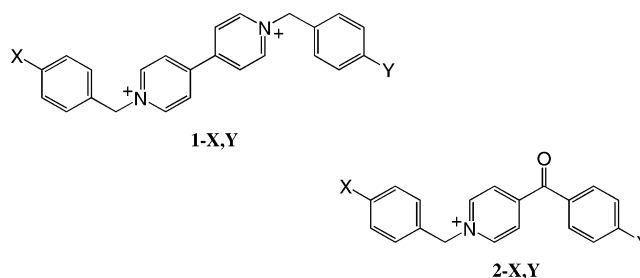
Substituents are selected from a design of experiments (DoE) perspective where both −X and −Y vary from strongly electron-withdrawing (−NO₂) to moderately strong electron-donating (−OCH₃). The effect of all *p*-benzyl substituents in both **1-X,Y** and **2-X,Y** is unambiguously inductive.[10] The effect of the

Electrochemical Reduction of **1-X,Y** and **2,X,Y**

J. Phys. Chem. B, Vol. 108, No. 30, 2004 **11229**

p-benzoyl substituents, −Y, in all **2-X,Y**'s is also expected to be purely inductive, because of the orthogonal geometry between the 4-benzoyl group and the two reduction sites of the 4-benzoylpyridinium system.[11] Half-wave potentials, $E_{1/2}$, were obtained experimentally and analyzed as a function of the substituent constants, σ_{p-X} and σ_{p-Y}. Multiple linear regressions confirm that the total substitution effect from the two groups is nonadditive.

Experimental Section

Electrochemical characterization by cyclic voltammtery was conducted as described before.[7,11] Experimental design and analysis was carried out using the RS/series for Windows, including RS/1 version 6.01, RS/Discover, and RS/Explore release 4.1, available from Domain Manufacturing Corporation, Burlington, MA.

Symmetric viologens **1-OCH₃,OCH₃**, **1-Br,Br**, and **1-NO₂,- NO₂** were prepared by quaternization of 4,4′-bipyridine with ∼2.5 equiv of the corresponding benzyl halide in acetonitrile under reflux for 24 h. Subsequently, the solvent was removed under reduced pressure, the solid was collected and dissolved in water, an aqueous solution containing 10 equiv of NH_4BF_4 was added, and the mixture was refluxed for 0.5 h. The mixture was cooled at ∼5 °C, and the precipitate was collected, recrystallized once from hot acetonitrile/methanol, and dried under vacuum.

***N,N′*-Di-(4-nitrobenzyl)-4,4′-bipyridinium Bistetrafluoroborate (1-NO₂,NO₂)** was prepared from 4,4′-dipyridyl (0.47 g, 0.003 mol) and 4-nitrobenzyl bromide (1.51 g, 0.007 mol).[12] Yield: 1.27 g (70% yield). mp: 268−270 °C. ¹H NMR (DMSO-d_6, 400 MHz): δ 6.08 (4H, s, −CH₂N⁺), 7.83 (4H, d, J = 8.42 Hz), 8.32 (4H, d, J = 8.42 Hz), 8.76 (4H, d, J = 6.60 Hz), 9.50 (4H, d, J = 6.60 Hz). ¹³C NMR (DMSO-d_6, 100 MHz): δ 62.4 (−CH₂N⁺), 124.2, 127.3, 130.3, 140.9, 146.2, 148.1, 149.5. Anal. calcd for $C_{24}H_{20}N_4O_4B_2F_8$: C, 47.88; H, 3.35; N, 9.31. Found: C, 47.87; H, 3.20; N, 9.06.

***N,N′*-Di-(4-bromobenzyl)-4,4′-bipyridinium Bistetrafluoroborate (1-Br,Br)** was prepared from 4,4′-dipyridyl (0.47 g, 0.003 mol) and 4-bromobenzyl bromide (1.75 g, 0.007 mol). Yield: 0.994 g (49%). mp: 300−302 °C. ¹H NMR (DMSO-d_6, 400 MHz): δ 5.89 (4H, s, −CH₂N⁺), 7.56 (4H, d, J = 8.42 Hz), 7.69 (4H, d, J = 8.42 Hz), 8.71 (4H, d, J = 6.59 Hz), 9.45 (4H, d, J = 6.59 Hz). ¹³C NMR (DMSO-d_6, 100 MHz): δ 62.7 (−CH₂N⁺), 123.1, 127.2, 131.3, 132.2, 133.4, 145.7, 149.3. Anal. calcd for $C_{24}H_{20}N_2Br_2B_2F_8$: C, 43.03; H, 3.01; N, 4.18. Found: C, 42.23; H, 2.80; N, 4.11.

***N,N′*-Di-(4-methoxylbenzyl)-4,4′-bipyridinium Bistetrafluoroborate (1-OCH₃,OCH₃)** was prepared from 4,4′-dipyridyl (0.94 g, 0.006 mol) and 4-methoxylbenzyl chloride (2.19 g, 0.014 mol).[13] Yield: 1.85 g (54%). mp: 248−250 °C. ¹H NMR (DMSO-d_6, 400 MHz): δ 3.75 (6H, s, −OCH₃), 5.82 (4H, s, −CH₂N⁺), 7.02 (4H, d, J = 8.51 Hz), 7.58 (4H, d, J = 8.51 Hz), 8.68 (4H, d, J = 6.77 Hz), 9.44 (4H, d, J = 6.77 Hz). ¹³C NMR (DMSO-d_6, 100 MHz): δ 55.3 (−OCH₃), 63.2 (−CH₂N⁺), 114.7, 126.0, 127.2, 130.8, 145.4, 149.2, 160.2. Anal. calcd for $C_{26}H_{26}N_2O_2B_2F_8$: C, 54.59; H, 4.58; N, 4.90. Found: C, 54.65; H, 4.10; N, 4.95.

Unsymmetric viologens **1-X,Y** were prepared as follows: a benzene solution of a substoichiometric amount of *p*-substituted halide (0.6 equiv) was added dropwise to a hot benzene solution of 4,4′-bipyridine under stirring. The mixture was refluxed for 6 h, and the precipitate was collected and washed with diethyl ether. The solid was dissolved in water, and the tetrafluoroborate salt was precipitated by adding an aqueous solution containing

a ∼6 equiv excess of NH_4BF_4. The mixture was cooled to ∼5 °C, and the monoquat product was collected and recrystallized once from methanol and once from water. Subsequently, 1 equiv of the monoquat was refluxed in acetonitrile with a 1.5 equiv of the appropriate benzyl halide for 24 h, and the reaction mixture was processed as in the case of the symmetric viologens above. Each final product was recrystallized once from hot methanol.

***N*-(4-Bromobenzyl)-*N′*-(4-nitrobenzyl)-4,4′-bipyridinium Bistetrafluoroborate (1-Br,NO₂)** was prepared from 4-bromobenzyl bromide (1.4 g, 0.006 mol) and 4,4′-dipyridyl (1.6 g, 0.01 mol) (first step), followed by the addition of 4-nitrobenzyl bromide (0.7 g, 0.003 mol) in the monoquat (0.83 g, 0.002 mol) (second step). Yield: 0.53 g (14%). mp: 264−266 °C. ¹H NMR (DMSO-d_6, 400 MHz): δ 5.90 (2H, s, −CH₂N⁺), 6.07 (2H, s, −CH₂N⁺), 7.56 (2H, d, J = 8.43 Hz), 7.70 (2H, d, J = 8.42 Hz), 7.83 (2H, d, J = 8.43 Hz), 8.32 (2H, d, J = 8.43 Hz), 8.72 (2H, d, J = 6.60 Hz), 8.76 (2H, d, J = 6.59 Hz), 9.46 (2H, d, J = 6.60 Hz), 9.49 (2H, d, J = 6.59 Hz). ¹³C NMR (DMSO-d_6, 100 MHz): δ 62.4 (−CH₂N⁺), 62.8 (CH₂N⁺), 123.2, 124.2, 127.3, 127.4, 130.3, 131.3, 132.3, 133.3, 140.9, 145.8, 146.1, 148.1, 149.3, 149.6. Anal. calcd for $C_{24}H_{20}N_2O_2BrB_2F_8$: C, 45.33; H, 3.17; N, 6.61. Found: C, 45.13; H, 3.03; N, 6.65.

***N*-(4-Bromobenzyl)-*N′*-(4-methoxybenzyl)-4,4′-bipyridinium Bistetrafluoroborate (1-Br,OCH₃)** was prepared from 4-bromobenzyl bromide (1.4 g, 0.006 mol) and 4,4′-dipyridyl (1.6 g, 0.01 mol) (first step), followed by the addition of 4-methoxybenzyl chloride (0.5 g, 0.003 mol) in the monoquat (0.83 g, 0.002 mol) (second step). Yield: 0.49 g (13%). mp: 244−245 °C. ¹H NMR (DMSO-d_6, 400 MHz): δ 3.75 (3H, s, −OCH₃), 5.83 (2H, s, −CH₂N⁺), 5.89 (2H, s, −CH₂N⁺), 7.01− 7.03 (2H, d, J = 8.80 Hz), 7.55−7.60 (4H, m), 7.67−7.71 (2H, m), 8.68−8.72 (4H, overlapping doublets), 9.44 (2H, d, J = 6.78 Hz). ¹³C NMR (DMSO-d_6, 100 MHz): δ 55.3 (−OCH₃), 62.7 (−CH₂N⁺), 63.2 (−CH₂N⁺), 114.7, 123.1, 125.9, 127.17, 127.24, 130.8, 131.3, 132.2, 133.4, 145.4, 145.7, 149.1, 149.4, 160.2. Anal. calcd for $C_{25}H_{23}N_2OBrB_2F_8$: C, 48.36; H, 3.73; N, 4.51. Found: C, 48.23; H, 3.40; N, 4.48.

***N*-(4-Nitrobenzyl)-*N′*-(4-methoxybenzyl)-4,4′-bipyridinium Bistetrafluoroborate (1-NO₂,OCH₃)** was prepared from 4-nitrobenzyl bromide (1.3 g, 0.006 mol) and 4,4′-dipyridinyl (1.6 g, 0.01 mol) (first step), followed by the addition of 4-methoxybenzyl chloride (0.6 g, 0.0037 mol) in the monoquat (0.91 g, 0.0024 mol) (second step). Yield: 0.60 g (18%). mp: 185−186 °C. ¹H NMR (DMSO-d_6, 400 MHz): δ 3.75 (3H, s, −OCH₃), 5.83 (2H, s, −CH₂N⁺), 6.06 (2H, s, −CH₂N⁺), 7.00 (2H, d, J = 8.61 Hz), 7.58 (2H, d, J = 8.61 Hz), 7.82 (2H, d, J = 8.42 Hz), 8.32 (2H, d, J = 8.42 Hz), 8.70 (2H, d, J = 6.78 Hz), 8.74 (2H, d, J = 6.78 Hz), 9.45 (2H, d, J = 6.78 Hz), 9.48 (2H, d, J = 6.78 Hz). ¹³C NMR (DMSO-d_6, 100 MHz): δ 55.3 (−OCH₃), 62.4 (−CH₂N⁺), 63.2 (−CH₂N⁺), 114.7, 124.2, 125.9, 127.2, 127.3, 130.3, 130.8, 140.9, 145.4, 146.1, 148.0, 149.0, 149.6, 160.2. Anal. calcd for $C_{25}H_{23}N_3O_3B_2F_8$: C, 51.15; H, 3.95; N, 7.16. Found: C, 50.86; H, 3.76; N, 7.06.

All **2-X,Y**'s were prepared by quaternization of 4-(*p*-substituted benzoyl) pyridine according to our previously described procedure.

4-*p*-Nitrobenzoyl-*N*-(4-nitrobenzyl)pyridinium Tetrafluoroborate (2-NO₂,NO₂) was prepared from 4-*p*-nitrobenzoylpyridine (3 g, 0.013 mol) and 4-nitrobenzyl bromide (6 g, 0.028 mol). Yield: 3.3 g (57%). mp: 205−207 °C. ¹H NMR (DMSO-d_6, 400 MHz): δ 6.11 (2H, s, −CH₂N⁺), 7.84−7.88 (2H, m), 8.07−8.11 (2H, m), 8.31−8.35 (2H, m), 8.39−8.43 (2H, m),

11230 *J. Phys. Chem. B, Vol. 108, No. 30, 2004*

Leventis et al.

8.46 (2H, d, $J = 6.78$ Hz), 9.44 (2H, d, $J = 6.78$ Hz). ^{13}C NMR (DMSO-d_6, 100 MHz): δ 62.6 ($-CH_2N^+$), 124.0, 124.2, 127.9, 130.4, 131.7, 139.1, 140.9, 146.4, 148.1, 150.5, 150.7, 191.0 (C=O). IR (KBr, cm^{-1}) 1680 (C=O). Anal. calcd for $C_{19}H_{14}N_3O_5BF_4$: C, 50.59; H, 3.13; N, 9.31. Found: C, 50.57; H, 3.24; N, 9.56.

4-*p*-Nitrobenzoyl-*N*-(4-bromobenzyl)pyridinium Tetrafluoroborate (2-Br,NO$_2$) was prepared from 4-*p*-nitrobenzoylpyridine (3 g, 0.013 mol) and 4-bromobenzyl bromide (6.5 g, 0.026 mol). Yield: 3.9 g (62%). mp: 146−148 °C. ^{1}H NMR (DMSO-d_6, 400 MHz): δ 5.92 (2H, s, $-CH_2N^+$), 7.56−7.60 (2H, m), 7.69−7.73 (2H, m), 8.08 (2H, d, $J = 8.79$ Hz), 8.38− 8.44 (4H, m), 9.40 (2H, d, $J = 6.59$ Hz). ^{13}C NMR (DMSO-d_6, 100 MHz): δ 63.6 ($-CH_2N^+$), 123.8, 124.6, 128.5, 132.1, 132.4, 132.9, 133.9, 139.8, 146.6, 151.1, 151.1, 191.0 (C=O). IR (KBr, cm^{-1}) 1681 (C=O). Anal. calcd for $C_{19}H_{14}N_2O_3$-BrBF$_4$: C, 47.05; H, 2.91; N, 5.78. Found: C, 46.54; H, 2.65; N, 5.72.

4-*p*-Nitrobenzoyl-*N*-(4-methoxybenzyl)pyridinium Tetrafluoroborate (2-OCH$_3$,NO$_2$) was prepared from 4-*p*-nitrobenzoylpyridine (3 g, 0.013 mol) and 4-methoxybenzyl chloride (4 g, 0.026 mol). Yield: 3.7 g (65%). mp: 92−94 °C. ^{1}H NMR (DMSO-d_6, 400 MHz): δ 3.77 (3H, s, $-OCH_3$), 5.86 (2H, s, $-CH_2N^+$), 7.01−7.05 (2H, m), 7.57−7.61 (2H, m), 8.05−8.09 (2H, m), 8.38−8.42 (4H, m), 9.38 (2H, d, $J = 6.78$ Hz). ^{13}C NMR (DMSO-d_6, 100 MHz): δ 55.3 ($-OCH_3$), 63.5 ($-CH_2N^+$), 114.7, 124.0, 125.8, 127.8, 131.1, 131.8, 139.2, 145.7, 150.2, 150.5, 160.3, 191.0 (C=O). IR (KBr, cm^{-1}) 1679 (C=O). Anal. calcd for $C_{20}H_{17}N_2O_4BF_4$: C, 55.08; H, 3.93; N, 6.42. Found: C, 54.96; H, 3.98; N, 6.21.

4-*p*-Methoxybenzoyl-*N*-(4-nitrobenzyl)pyridinium Tetrafluoroborate (2-NO$_2$,OCH$_3$) was prepared from 4-*p*-methoxybenzoylpyridine (3 g, 0.014 mol) and 4-nitrobenzyl bromide (6 g, 0.028 mol). Yield: 4.1 g (67%). mp: 174−176 °C. ^{1}H NMR (DMSO-d_6, 400 MHz): δ 3.88 (3H, s, $-OCH_3$), 6.07 (2H, s, $-CH_2N^+$), 7.12−7.16 (2H, m), 7.82−7.87 (4H, m), 8.31−8.34 (2H, m), 8.39 (2H, d, $J = 6.78$ Hz), 9.38 (2H, d, $J = 6.59$ Hz). ^{13}C NMR (DMSO-d_6, 100 MHz): δ 55.9 ($-OCH_3$), 62.4 ($-CH_2N^+$), 114.5, 124.2, 126.9, 127.3, 130.4, 133.1, 141.0, 146.1, 148.0, 153.1, 164.7, 190.4 (C=O). IR (KBr, cm^{-1}) 1656 (C=O). Anal. calcd for $C_{20}H_{17}N_2O_4BF_4$: C, 55.08; H, 3.93; N, 6.42. Found: C, 54.44; H, 3.85; N, 6.26.

4-*p*-Methoxybenzoyl-*N*-(4-bromobenzyl)pyridinium Tetrafluoroborate (2-Br,OCH$_3$) was prepared from 4-*p*-methoxybenzoylpyridine (3 g, 0.014 mol) and 4-bromobenzyl bromide (7 g, 0.028 mol). Yield: 5.0 g (77%). mp: 154−156 °C. ^{1}H NMR (DMSO-d_6, 400 MHz): δ 3.88 (3H, s, $-OCH_3$), 5.89 (2H, s, $-CH_2N^+$), 7.11−7.15 (2H, m), 7.56−7.60 (2H, m), 7.68−7.72 (2H, m), 7.81−7.85 (2H, m), 8.35 (2H, d, $J = 6.59$ Hz), 9.34 (2H, d, $J = 6.78$ Hz). ^{13}C NMR (DMSO-d_6, 100 MHz): δ 55.9 ($-OCH_3$), 62.8 ($-CH_2N^+$), 114.5, 123.1 126.9, 127.2, 131.5, 132.2, 133.1, 133.2, 145.8, 152.8, 164.6, 190.4 (C=O). IR (KBr, cm^{-1}) 1659 (C=O). Anal. calcd for $C_{20}H_{17}$-NO$_2$BrBF$_4$: C, 51.10; H, 3.65; N, 2.98. Found: C, 51.37; H, 3.45; N, 2.87.

4-*p*-Methoxybenzoyl-*N*-(4-methoxybenzyl) Pyridinium Tetrafluoroborate, (2-OCH$_3$,OCH$_3$) was prepared from 4-*p*-methoxybenzoylpyridine (3 g, 0.014 mol) and 4-methoxybenzyl chloride (4.3 g, 0.028 mol). Yield: 3.2 g (53%). mp: 135− 137 °C. ^{1}H NMR (DMSO-d_6, 400 MHz): δ 3.76 (3H, s, $-OCH_3$), 3.88 (3H, s, $-OCH_3$), 5.83 (2H, s, $-CH_2N^+$), 7.01− 7.05 (2H, m), 7.11−7.15 (2H, m), 7.57−7.61 (2H, m), 7.80− 7.84 (2H, m), 8.32 (2H, d, $J = 6.59$ Hz), 9.32 (2H, d, $J = 6.77$ Hz). ^{13}C NMR (DMSO-d_6, 100 MHz): δ 55.3 ($-OCH_3$), 55.9

($-OCH_3$), 63.2 ($-CH_2N^+$), 114.5, 114.7 125.8, 126.9, 127.1, 131.1, 133.0, 145.4, 152.6, 160.2, 164.6, 190.4 (C=O). IR (KBr, cm^{-1}) 1658 (C=O). Anal. calcd for $C_{21}H_{20}NO_3BF_4$: C, 59.88; H, 4.79; N, 3.33. Found: C, 59.49; H, 4.36; N, 3.25.

4-*p*-Bromobenzoyl-*N*-(4-nitrobenzyl)pyridinium Tetrafluoroborate (2-NO$_2$,Br) was prepared from 4-*p*-bromobenzoylpyridine (3 g, 0.0115 mol) and 4-nitrobenzyl bromide (5 g, 0.023 mol). Yield: 4.5 g (82%). mp: 162−163 °C. ^{1}H NMR (DMSO-d_6, 400 MHz): δ 6.08 (2H, s, $-CH_2N^+$), 7.76−7.80 (2H, m), 7.83−7.87 (4H, m), 8.31−8.34 (2H, m), 8.42 (2H, d, $J = 6.80$ Hz), 9.41 (2H, d, $J = 6.80$ Hz, H-10,12). ^{13}C NMR (DMSO-d_6, 100 MHz): δ 62.5 ($-CH_2N^+$), 124.2, 127.7, 129.3, 130.4, 132.2, 132.3, 133.3, 140.9, 146.3, 148.0, 151.6, 191.3 (C=O). IR (KBr, cm^{-1}) 1665 (C=O). Anal. calcd for $C_{19}H_{14}N_2O_3BrBF_4$: C, 47.05; H, 2.91; N, 5.78. Found: C, 47.27; H, 2.96; N, 5.56.

4-*p*-Bromobenzoyl-*N*-(4-bromobenzyl)pyridinium Tetrafluoroborate (2-Br,Br) was prepared from 4-*p*-bromobenzoylpyridine (3 g, 0.0115 mol) and 4-bromobenzyl bromide (6 g, 0.024 mol). Yield: 4.7 g (79%). mp: 191−193 °C. ^{1}H NMR (DMSO-d_6, 400 MHz): δ 5.89 (2H, s, $-CH_2N^+$), 7.55−7.59 (2H, m), 7.67−7.71 (2H, m), 7.74−7.79 (2H, m), 7.81−7.85 (2H, m), 8.37 (2H, d, $J = 6.59$ Hz), 9.36 (2H, d, $J = 6.78$ Hz). ^{13}C NMR (DMSO-d_6, 100 MHz): δ 62.8 ($-CH_2N^+$), 123.1, 127.6, 129.2, 131.5, 132.18, 132.21, 132.24, 133.2, 133.3, 145.9, 151.4, 191.3 (C=O). IR (KBr, cm^{-1}) 1670 (C=O). Anal. calcd for $C_{19}H_{14}NOBr_2BF_4$: C, 43.98; H, 2.72; N, 2.70. Found: C, 43.88; H, 2.60; N, 2.65.

4-*p*-Bromobenzoyl-*N*-(4-methoxybenzyl)pyridinium Tetrafluoroborate (2-OCH$_3$,Br) was prepared from 4-*p*-bromobenzoylpyridine (3 g, 0.0115 mol) and 4-methoxybenzyl chloride (3.6 g, 0.023 mol). Yield: 4.7 g (79%). mp: 171−173 °C. ^{1}H NMR (DMSO-d_6, 400 MHz): δ 3.76 (3H, s, $-OCH_3$), 5.84 (2H, s, $-CH_2N^+$), 7.01−7.05 (2H, m), 7.56−7.61 (2H, m), 7.74−7.78 (2H, m), 7.82−7.86 (2H, m), 8.36 (2H, d, $J = 6.60$ Hz), 9.35 (2H, d, $J = 6.60$ Hz). ^{13}C NMR (DMSO-d_6, 100 MHz): δ 55.3 ($-OCH_3$), 63.3 ($-CH_2N^+$), 114.6, 125.7, 127.5, 129.2, 131.0, 132.17, 132.22, 133.3, 145.5, 151.1, 160.2, 191.3 (C=O). IR (KBr, cm^{-1}) 1666 (C=O). Anal. calcd for $C_{20}H_{17}$-NO$_2$BrBF$_4$: C, 51.10; H, 3.64; N, 2.98. Found: C, 51.02; H, 3.46; N, 2.97.

Results and Discussion

Of the very large number of possible groups for $-X$ and $-Y$,[14] we have concentrated on those available from our previous studies as substituents either of the *p*-X-benzyl halides used for quaternization of 4-benzoylpyridine (six compounds)[7] or of 4-(*p*-Y-benzoyl) pyridine (nine compounds).[11a] These groups vary from strong electron acceptors (e.g., $-NO_2$) to moderately strong electron donors (e.g., $-OCH_3$). To evaluate the effect of substitution on an unsymmetric system such as **2-X,Y**, using all of our *p*-X-benzyl halides and 4-(*p*-Y-benzoyl) pyridines would require preparation of a large number of compounds (54). It is possible, however, to evaluate the effects of multiple substitution by using only three carefully chosen substituents with high, medium, and low substituent constants (e.g., $\sigma_{p-NO_2} = 0.78$, $\sigma_{p-Br} = 0.26$, and, $\sigma_{p-OCH_3} = -0.27$). Thus, considering σ_{p-X} and σ_{p-Y} as two independent, continuous variables at three levels each, a full-factorial experimental design strategy can be employed using only nine compounds.[15] In the case of viologens, because of symmetry, **1-X,Y**'s are equivalent to **1-Y,X**'s. Therefore, again utilizing three levels for σ_{p-X} and σ_{p-Y}, the number of possible different compounds is only six.

The synthesis of the nine compounds was straightforward and was carried out by simple quaternization of 4,4′-bipyridine or

4-(p-Y-benzoyl) pyridine with the appropriate p-X-benzyl halides. All nine **2-X,Y**'s as well as **1-NO₂,Br**, **1-Br,Br**, **1-OCH₃,NO₂**, and **1-OCH₃,Br** are new compounds. Detailed compound characterization is given in the Experimental Section.

Redox characterization of all compounds was conducted with cyclic voltammetry in CH₃CN/0.1 M TBAP at 0.1 V s⁻¹, whenever possible (see below). All voltammograms are compensated for solution resistance and are referenced internally to ferrocene.[7,11,16] The results are summarized in Table 1 for **1-X,Y**'s and in Table 2 for **2-X,Y**'s. Typical voltammograms are shown in Figure 1.

All **1-X,Y**'s show two reversible 1-e waves from the diquaternized 4,4′-bipyridinium core (Figure 1A). **1-X,NO₂**-type compounds show a third wave (Figure 1B), which is attributed to the reduction of the nitrobenzyl group itself.[7,11a,16] Since this reduction takes place at more negative potentials than the reduction of the 4,4′-bipyridinium, it does not interfere with it. Interestingly, reduction of the two nitro groups in **1-NO₂,NO₂** yields a 1-e wave twice the size with practically no increase in the $\Delta E_{1/2}$ value, meaning that there is no significant electronic communication between the two groups.

Compounds **2-X,Y**'s with no −NO₂ substituents also yield two reversible waves at 0.1 V s⁻¹ (Figure 1A). (With regard to reversibility, note that the ΔE_{p-p} values are consistently smaller than the corresponding values for ferrocene.) In **2-NO₂,Y** or **2-X,NO₂** the reduction of the nitro group now falls between the first- and the second-e reduction of the 4-benzoyl-N-benzyl pyridinium system. This affects the reversibility of the second-e reduction of the 4-benzoyl-N-benzyl pyridinium system, which now appears reversible only at high sweep rates (e.g., 5 or 10 V s⁻¹).[7] (In the case of **2-NO₂,NO₂**, only the first reduction is reversible; the rest of the reduction waves are not reversible even for sweep rates up to ∼66 V s⁻¹.) Upon reduction, −NO₂ is converted to −NO₂•⁻, a very strong electron donor pushing the third wave (corresponding to the second-e reduction of the **2-X,Y** system) to more negative potentials.[17] This phenomenon is more pronounced in the case of **2-OCH₃,NO₂** (dots) than in the case of **2-NO₂,Br** (dashes), because in the former case the −NO₂ group is attached directly on the redox system.

Half wave potentials, $E_{1/2}$'s, were calculated from the cathodic and anodic peak current potentials, $E_{p,c}$ and $E_{p,a}$, respectively, according to $E_{1/2} = (E_{p,c} + E_{p,a})/2$, and were analyzed by multiple-linear least squares regression in terms of σ_{p-X} and σ_{p-Y}.[15] Thus, following Wold's approach,[18] the general extrathermodynamic function that describes the dependence of $E_{1/2}$ on σ_{p-X} and σ_{p-Y}, $E_{1/2} = F(\sigma_{p-X}, \sigma_{p-Y})$, is expanded into a Taylor series around any arbitrary data point, such as for example $(\sigma_{p-X=H}, \sigma_{p-Y=H}) = (0,0)$. This process yields eq 1, where $[F'_{\sigma_{p-X}}]$ represents the first derivative of $F(\sigma_{p-X}, \sigma_{p-Y})$ with respect to σ_{p-X}

$$E_{1/2} = [F(0,0)] + [F'_{\sigma_{p-X}}]\sigma_{p-X} + [F'_{\sigma_{p-Y}}]\sigma_{p-Y} + (1/2)$$
$$[F''_{\sigma_{p-X}, \sigma'_{p-X}}](\sigma_{p-X})^2 + [F''_{\sigma_{p-X}, \sigma_{p-Y}}](\sigma_{p-X}\sigma_{p-Y}) + (1/2)$$
$$[F''_{\sigma_{p-Y}, \sigma_{p-Y}}](\sigma_{p-Y})^2 + R(3) \quad (1)$$

evaluated at the limit of $(\sigma_{p-X}, \sigma_{p-Y}) = (0,0)$, and so forth. The residue R(3) contains terms of third order and higher and a term due to experimental error. According to eq 1, a full quadratic model was entertained, including second-order effects and synergistic/interactive effects between σ_{p-X} and σ_{p-Y}. Terms below the 90% confidence limit were not deemed statistically significant and were dropped from the model using a stepwise regression technique.

TABLE 1: Electrochemical Data for N,N′-(p-Substituted benzyl)viologens (1-X,Y)[a]

compound	$E_{1/2}(1)$	$\Delta E_{p-p}(1)$	$i_{p,c}/i_{p,a}(1)$	$E_{1/2}(2)$	$\Delta E_{p-p}(2)$	$i_{p,c}/i_{p,a}(2)$	$E_{1/2}(3)$	$\Delta E_{p-p}(3)$	$i_{p,c}/i_{p,a}(3)$	$E_{1/2}(Fc)^b$	$\Delta E_{p-p}(Fc)$
1-Br,Br	−0.742 ± 0.000	67 ± 3	1.00	−1.137 ± 0.004	65 ± 2	1.11	–	–	–	0.433 ± 0.001	68 ± 1
1-OCH₃,OCH₃	−0.780 ± 0.001	66 ± 1	1.00	−1.187 ± 0.001	61 ± 3	1.15	–	–	–	0.431 ± 0.001	72 ± 2
1-OCH₃,Br	−0.761 ± 0.001	64 ± 2	1.00	−1.164 ± 0.001	64 ± 1	1.16	–	–	–	0.436 ± 0.001	69 ± 2
1-Br,NO₂	−0.723 ± 0.001	67 ± 3	1.00	−1.115 ± 0.000	65 ± 2	1.07	−1.529 ± 0.001	75 ± 3	1.08	0.434 ± 0.001	73 ± 1
1-OCH₃,NO₂	−0.743 ± 0.001	73 ± 2	0.96	−1.139 ± 0.002	66 ± 4	1.14	−1.533 ± 0.003	86 ± 9	1.00	0.436 ± 0.000	76 ± 0
1-NO₂,NO₂	−0.703 ± 0.001	69 ± 1	1.03	−1.093 ± 0.001	68 ± 3	1.10	−1.538 ± 0.001	90 ± 3	1.02	0.431 ± 0.001	79 ± 1

[a] Determined with ∼3 mM solutions of **1-X,Y**s in Ar degassed, 80% resistance compensated CH₃CN/0.1 M TBAP, at 0.1 V s⁻¹. Data are averages of three voltammograms. $E_{1/2}$ values are reported versus ferrocene (Fc) included as an internal standard. [b] $E_{1/2}$(Fc) values are reported vs the Ag/AgCl reference electrode.

TABLE 2: Electrochemical Data for 4-(p-Substituted benzoyl)-N-(p-substituted Benzyl) Pyridinium Cations (2-X,Y)[a]

compound	$E_{1/2}(1)$[b]	$\Delta E_{p-p}(1)$	$i_{p,c}/i_{p,a}(1)$	$E_{1/2}(2)$	$\Delta E_{p-p}(2)$	$i_{p,c}/i_{p,a}(2)$	$E_{1/2}(3)$	$\Delta E_{p-p}(3)$	$i_{p,c}/i_{p,a}(3)$	$E_{1/2}$ (Fc)[g]	ΔE_{p-p}(Fc)
2-OCH₃,OCH₃	−1.086 ± 0.001	67 ± 2	1.02	−1.704 ± 0.005[b]	71 ± 1	1.11	—	—	—	0.455 ± 0.000[b]	74 ± 0
2-OCH₃,Br	−0.998 ± 0.000	71 ± 1	1.04	−1.594 ± 0.001[b]	73 ± 1	1.04	—	—	—	0.452 ± 0.000[b]	76 ± 0
2-Br,Br	−0.972 ± 0.002	66 ± 3	1.09	−1.606 ± 0.000[b]	71 ± 1	1.14	—	—	—	0.455 ± 0.001[b]	75 ± 1
2-Br,OCH₃	−1.061 ± 0.001	68 ± 1	1.00	−1.646 ± 0.001[b]	77 ± 1	1.10	—	—	—	0.458 ± 0.000[b]	75 ± 2
2-OCH₃,NO₂	−0.916 ± 0.003	69 ± 3	1.10	−1.347 ± 0.002[c]	77 ± 1	0.93	−1.860 ± 0.004[c]	92 ± 4	1.10	0.454 ± 0.002[c]	85 ± 3
2-Br,NO₂	−0.896 ± 0.001	70 ± 1	1.06	−1.345 ± 0.001[c]	74 ± 1	1.00	−1.810 ± 0.001[c]	79 ± 1	1.35	0.458 ± 0.000[c]	72 ± 0
2-NO₂,Br	−0.949 ± 0.001	68 ± 1	1.02	−1.489 ± 0.004[d]	89 ± 9	f	−1.639 ± 0.002[d]	107 ± 14	f	0.459 ± 0.001[d]	95 ± 11
2-NO₂,OCH₃	−1.036 ± 0.001	67 ± 1	1.26	−1.491 ± 0.017[d]	69 ± 3	f	−1.707 ± 0.003[d]	102 ± 0	f	0.457 ± 0.001[d]	75 ± 2
2-NO₂,NO₂	−0.873 ± 0.004	67 ± 6	1.27	e	e	e	e	e	e	0.453 ± 0.004	68 ± 7

[a] All conditions as in Table 1, unless noted otherwise. [b] At 0.1 V s⁻¹. [c] At 5 V s⁻¹. [d] At 10 V s⁻¹. [e] Irreversible up to 66 V s⁻¹. [f] Merging waves; the baseline current could not be established. [g] $E_{1/2}$(Fc) values are reported vs the Ag/AgCl reference electrode.
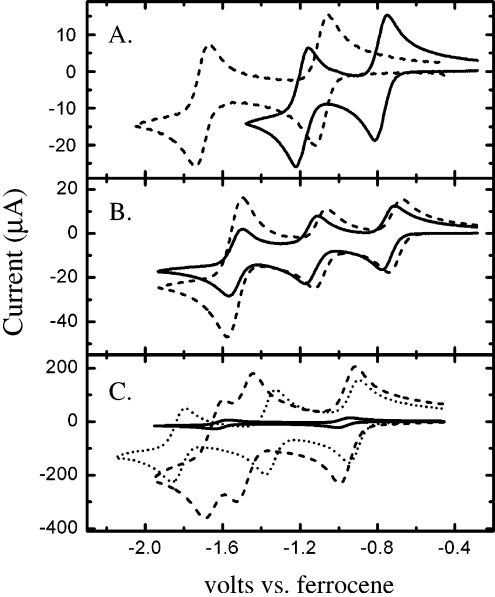

Figure 1. (A) Cyclic voltammetry (CV) of **1-OCH₃,OCH₃** (—, 3.16 mM) and of **2-OCH₃,OCH₃** (− − −, 3.06 mM) at 0.1 V s⁻¹. (B) CV of **1-OCH₃NO₂** (—, 2.83 mM) and of **1-NO₂,NO₂** (− − −, 3.02 mM) at 0.1 V s⁻¹. (C) CV of **2-Br,Br** (—, 3.30 mM) at 0.1 V s⁻¹, of **2-NO₂,-Br** (− − −, 3.75 mM) at 5 V s⁻¹ and of **2-OCH₃,NO₂** (···, 2.98 mM) at 10 V s⁻¹. All voltammograms were obtained in Ar-degassed CH₃-CN/0.1 M TBAP solutions with a Au-disk electrode (0.0201 cm²).

TABLE 3: Least-Squares Analysis of the $E_{1/2}$ Data Shown in Figure 2 for 1-X,Y[17]

variable in eq 1	corresponding coefficient	
	for $E_{1/2}(1)$, V	for $E_{1/2}(2)$, V
1	−0.760₈	−1.161₁
σ_{p-X}	0.035₅	0.051₆
σ_{p-Y}	0.036₀	0.043₅
$\sigma_{p-X}\,\sigma_{p-Y}$	−0.003₂	−0.009₅
error analysis		
R^2	1.0000	0.9997
RMS error (V)	0.000235	0.000914

Figure 2, parts A and B, shows the response surface models, and Table 3 summarizes the significant terms and relevant statistical data for the first- and the second-e reduction of **1-X,Y**'s. Dark circles in Figure 2 represent the data used for the regression. Light circles represent the data points if the positions of −X and −Y were considered reversed (due to symmetry). As expected, these new points also fit the same response surface model. Clearly, the response surface models represent three-dimensional Hammett plots.

Figure 3 shows the response surface models for the first- and the second-e reduction of **2-X,Y**'s.[17] Dark circles represent data obtained with the **2-X,Y** compounds in Table 2, while open circles correspond to data obtained previously under similar conditions for various **2-X,H**, i.e., for **2-X,Y** compounds where −Y = −H.[7] Table 4 summarizes the significant terms of the corresponding quadratic model. Thus, the top half of Table 4 summarizes the statistics using only the new data of Table 2 (dark circles in Figure 3) and the bottom half summarizes the statistics using both the data from Table 2 as well as the data from ref 7 for our six **2-X,H**'s. The new binary variable "block" shown in the bottom half of Table 4 is introduced in the model of eq 1 and is set equal to R(3) in order to detect and account for systematic errors between the two sets (blocks) of data,
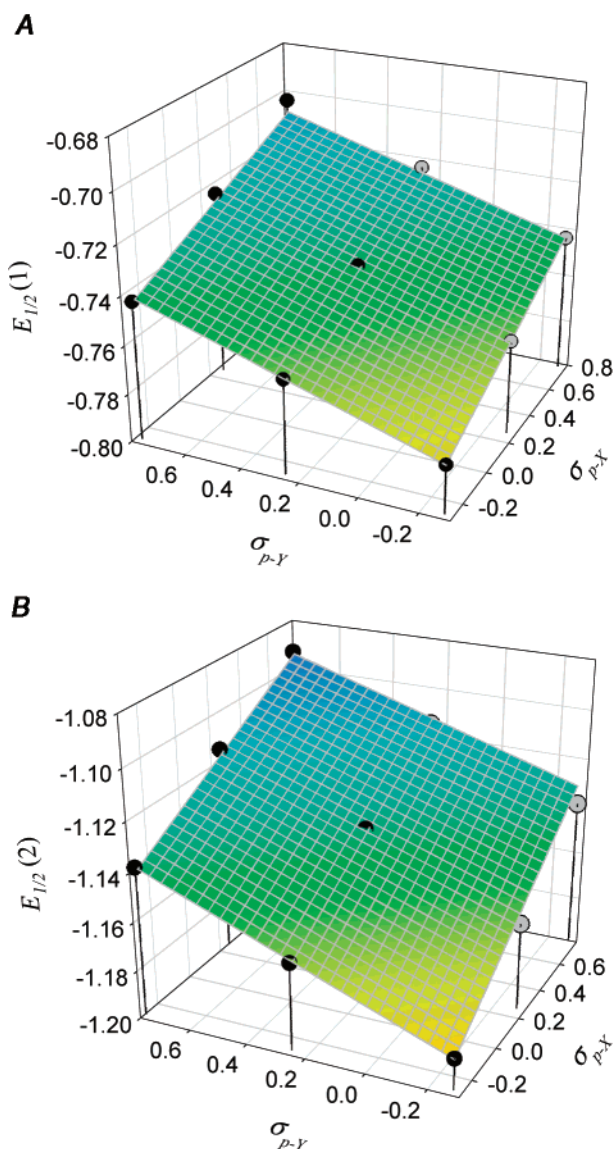
A

B

Figure 2. Response surface models for the $E_{1/2}(1)$ (A) and the $E_{1/2}(2)$ (B) of **1-X,Y**'s according to eq 1. For the raw data (dark circles), see Table 1. (Light circles correspond to **1-Y,X**'s, which, because of symmetry are identical to **1-X,Y**'s.) For the statistical analysis of the nonlinear regression, see Table 3.

arising for example from the fact that they were obtained at different times by different experimenters. In this regard, an improvement (i.e., an increase) in the correlation coefficient and a decrease in the RMS error of the response surface indicates a systematic error that, for example, results in a parallel displacement of the surface segment describing the "block" of data. This is clearly the case with the $E_{1/2}(2)$ values in Table 4B (vide infra) where "block" is a significant term in both the $E_{1/2}(1)$ and $E_{1/2}(2)$ models with 99.99% confidence.

According to the data of Table 3, the effect of substitution on the values of the $E_{1/2}(1)$ and $E_{1/2}(2)$ (in volts) for the first- and the second-e reductions of **1-X,Y**'s are given by eqs 2 and 3, respectively:

$$E_{1/2}(1) = -0.761 + 0.036\sigma_{\text{p}-\text{X}} + 0.036\sigma_{\text{p}-\text{Y}} - 0.003\,\sigma_{\text{p}-\text{X}}\sigma_{\text{p}-\text{Y}} \quad (2)$$

$$E_{1/2}(2) = -1.161 + 0.052\sigma_{\text{p}-\text{X}} + 0.044\sigma_{\text{p}-\text{Y}} - 0.010\sigma_{\text{p}-\text{X}}\sigma_{\text{p}-\text{Y}} \quad (3)$$
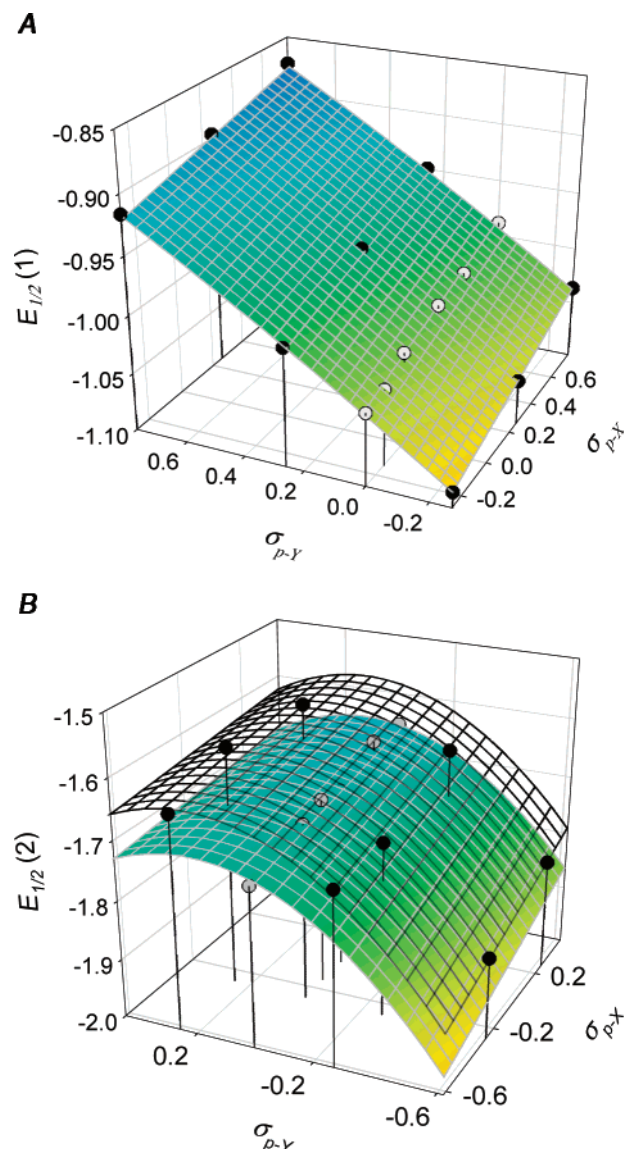
A

B

Figure 3. Response surface models for the $E_{1/2}(1)$ (A) and the $E_{1/2}(2)$ (B) of **2-X,Y**'s according to eq 1. For the new raw data (dark circles, upper surface), see Table 2. Light circles (lower surface) correspond to data for **2-X,H**'s taken from ref 7. For the statistical analysis of the nonlinear regression see the bottom half of Table 4.

According to the data of the top half of Table 4, the effect of substitution on the values of the $E_{1/2}(1)$ and $E_{1/2}(2)$ (in volts) for the first- and the second-e reductions of **2-X,Y**'s are given by eqs 4 and 5, respectively:

$$E_{1/2}(1) = -1.027 + 0.047\sigma_{\text{p}-\text{X}} + 0.168\sigma_{\text{p}-\text{Y}} - 0.006\sigma_{\text{p}-\text{X}}\sigma_{\text{p}-\text{Y}} - 0.015(\sigma_{\text{p}-\text{Y}})^2 \quad (4)$$

$$E_{1/2}(2) = -1.610 + 0.059\sigma_{\text{p}-\text{X}} + 0.133\sigma_{\text{p}-\text{Y}} - 0.368(\sigma_{\text{p}-\text{Y}})^2 \quad (5)$$

whereas according to the data of the bottom half of Table 4, the effect of substitution is given correspondingly by eqs 6 and 7, where the final constant is the "block" term.

$$E_{1/2}(1) = -1.025 + 0.047\sigma_{\text{p}-\text{X}} + 0.168\sigma_{\text{p}-\text{Y}} - 0.007\sigma_{\text{p}-\text{X}}\sigma_{\text{p}-\text{Y}} - 0.015\,(\sigma_{\text{p}-\text{Y}})^2 \pm 0.002 \quad (6)$$

$$E_{1/2}(2) = -1.644 + 0.061\sigma_{\text{p}-\text{X}} + 0.120\sigma_{\text{p}-\text{Y}} - 0.064\sigma_{\text{p}-\text{X}}\sigma_{\text{p}-\text{Y}} - 0.396(\sigma_{\text{p}-\text{Y}})^2 \pm 0.037 \quad (7)$$

TABLE 4: Least-Squares Analysis of the $E_{1/2}$ Data Shown in Figure 3 for 2-X,Y[17]

Analysis of the $E_{1/2}$ Data from Table 2 ($-Y \neq -H$)

	corresponding coefficient	
variable in eq 1	for $E_{1/2}(1)$, V	for $E_{1/2}(2)$, V
1	-1.027_1	-1.610_4
σ_{p-X}	0.046_7	0.058_9
σ_{p-Y}	0.167_5	0.133_4
$\sigma_{p-X}\sigma_{p-Y}$	-0.006_3	
$(\sigma_{p-Y})^2$	-0.015_3	-0.368_2
error analysis		
R^2	0.9999	0.9769
RMS error (V)	0.001141	0.01927

Analysis of the $E_{1/2}$ Data from Table 2 ($-Y \neq -H$) and from Ref 7 ($-Y = -H$)

	corresponding coefficient	
variable in eq 1	for $E_{1/2}(1)$, V	for $E_{1/2}(2)$, V
1	-1.025_4	-1.644_5
σ_{p-X}	0.046_8	0.060_9
σ_{p-Y}	0.167_5	0.119_6
$\sigma_{p-X}\sigma_{p-Y}$	-0.006_5	-0.064_4
$(\sigma_{p-Y})^2$	-0.015_3	-0.396_2
block new data[a]	0.001_7	0.036_5
old data[b]	-0.001_7	-0.036_5
error analysis		
R^2	0.9992	0.9785
RMS error (V)	0.002163	0.01361

[a] Data from Table 2. [b] Data from ref 7.

In the case of viologens (**1-X,Y**), all experimental points in both response surfaces for $E_{1/2}(1)$ and $E_{1/2}(2)$ fall very close to the best fits, and the correlation coefficients are exceptionally high ($R^2 \geq 0.9997$). As we have shown recently, by dividing the Hammett slope of a redox reaction by 0.059 V (for 1-e processes), one obtains the dimensionless reaction constant, ρ, which allows comparison of the redox reaction with any other kind of reaction susceptible to substitution effects.[11a] Thus, the coefficients of the linear terms being less than 0.059 V correspond to ρ values less than unity and reflect the separation of the reduction sites from the substituted aromatic systems by methylene groups.[10] The coefficients of the nonlinear terms vary between 8 and 20% of those for the linear terms. Although their effect is small (3 ± 1 mV and 10 ± 4 mV for $E_{1/2}(1)$ and $E_{1/2}(2)$, respectively; Table 3), they are statistically significant over and above the root mean square (RMS) error of the regression (≤ 1 mV, Table 3), and therefore they are clearly discernible.

In the case of the 4-(Y-benzoyl)-N-(X-benzyl)pyridinium cations (**2-X,Y**), again because of the presence of the $-CH_2-$ spacers, the coefficients of all σ_{p-X} terms in eqs 4–7 are ~0.059 V or less and correspond to reaction constants, ρ, less than unity. On the other hand, the coefficients of the second linear term, σ_{p-Y}, correspond to ρ values in the range 2 to 3, reflecting the fact that p-benzoyl substituents, although not in conjugation with the reduction site (with the exception of $-OCH_3$; see below),[11a] they nevertheless transmit their electronic properties effectively through the highly polarizable π-system over longer distances, and thus they are felt closer to the reduction sites. As far as nonlinear effects are concerned, using the data of Table 2 only (dark circles in Figure 3), nonlinear terms are encountered in the response surface of both $E_{1/2}(1)$'s and $E_{1/2}(2)$'s (see eqs 4 and 5). Thus, in the case of $E_{1/2}(1)$'s we note two nonlinear terms with coefficients equal to 6 mV for the interactive term ($\sigma_{p-X}\sigma_{p-Y}$) and 15 mV for the square term ($\sigma_{p-Y})^2$, both

statistically significant with >90% confidence over and above the RMS error of the regression (1 mV, Table 4, top half). For the response surface of $E_{1/2}(2)$'s, the standard error is 1 order of magnitude greater (19.3 mV), and only the square term ($\sigma_{p-Y})^2$ is statistically significant.

What renders the response surface of $E_{1/2}(2)$'s higher in error is probably related to the fact that five of the nine **2-X,Y**'s of Table 2 include the $-NO_2$ group. This group is reduced before the second-e reduction of the 4-benzoylpyridinium system itself (Figure 1C) and thus changes the character of the substituent from a strong electron acceptor ($-NO_2$) to a strong electron donor ($-NO_2^{\bullet-}$), creating an uncertainty with respect to the substituent constant,[17] while it also renders the second-e reduction of the 4-benzoylpyridinium system irreversible at slow sweep rates. At higher sweep rates (e.g., 5 or 10 V s^{-1}), all waves except that for **2-NO₂,NO₂** appear reversible, but higher sweep rates in cyclic voltammetry also produce higher currents, which, in combination with the remaining uncompensated solution resistance, shift the experimental values of $E_{1/2}(2)$ away from their true values.
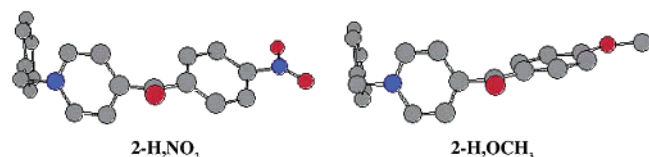
In a first effort to decrease the RMS error of the $E_{1/2}(2)$ surface, it was deemed reasonable to enlarge the data set used in the nonlinear regression (Table 2) by including data from our previous work with **2-X,H**'s. Using the behavior of the $E_{1/2}(1)$ as a gauge for the reliability of this operation, our data set enlargement changes eq 4 into

$$E_{1/2}(1) = -1.025 + 0.045\sigma_{p-X} + 0.168\sigma_{p-Y} - 0.022(\sigma_{p-Y})^2$$

whereas one of the nonlinear terms has disappeared. Simultaneously, the correlation coefficient is reduced from 0.9999 to 0.9984, and the RMS error is increased from 1.1 to 2.7 mV. On the other hand, using the "block" variable together with the same two data sets leaves the results from the regression analysis practically unchanged (compare the $E_{1/2}(1)$ coefficients in the top and bottom halves of Table 4). In this case, "block" is very small (only 2 mV) but highly statistically significant (99.99% confidence).

In the case of $E_{1/2}(2)$, combining the two data sets without using "block" changes eq 5 to $E_{1/2}(2) = -1.658 + 0.035\sigma_{p-X} + 0.174\sigma_{p-Y}$ with $R^2 = 0.8742$ and gives an RMS error of 28 mV, masking all nonlinear effects. Use of the "block" variable improves the correlation coefficient to $R^2 = 0.9785$ (Table 4, bottom half) and reduces the RMS error to 13.6 mV, rendering two nonlinear terms statistically significant (compare eqs 5 and 7).

From a chemical perspective, cross-product nonlinear terms indicate that substitution at one site renders the molecule disproportionally more (or less) susceptible to the effects of substitution at the second site; square nonlinear terms indicate that substituents of one type (e.g., electron donors) influence the molecule differently from substituents of a second type (e.g., electron acceptors). For example, in the case of the reaction of aryl benzoates with anionic nucleophiles,[2] it was proposed that electron-donating substituents on the benzoyl moiety interact with and stabilize through resonance the reacting carbonyl group, causing the Hammett plot to curve down. Similar "curving down" is observed with both the **1-X,Y**'s and the **2-X,Y**'s of this study (note that the coefficients of all nonlinear terms are negative). Thus, in analogy to reasoning set forth in ref 2, the reacting group in the second-e reduction of the 4-benzoylpyridinium system (**2-X,Y**'s) is also the carbonyl, which is in direct conjugation with electron-donating substituents such as the

Electrochemical Reduction of **1-X,Y** and **2,X,Y**

J. Phys. Chem. B, Vol. 108, No. 30, 2004 **11235**

CHART 1: PM3 Results for 2-H,NO₂ and 2-H,OCH₃

2-H,NO₂

2-H,OCH₃

−OCH₃ group. Therefore, the coefficients of the nonlinear terms increase dramatically (refer to eq 7). On the other hand, with regard to the first-e reduction of **2-X,Y**'s, PM3 semiempirical calculations show that as −Y becomes more electron donating, the benzoyl group becomes more planar (the dihedral angle between the aryl group and the carbonyl decreases from 38.7° to 0.8° by going from −Y = −NO₂ to −Y = −OCH₃; refer to Chart 1). Thus, the resonance interaction increases between −OCH₃ and the carbonyl group. (This resonance interaction is reflected clearly by the lower IR C=O stretching frequencies for −Y = −OCH₃ (1656−1659 cm⁻¹) than for −Y = −NO₂ (1679−1681 cm⁻¹); see also Experimental Section.) And, although there is still no resonance interaction between −Y and the pyridinium group that is reduced in the first-e reduction (note that the dihedral angle between the pyridinium and the carbonyl is ∼88°), nevertheless the near-planar geometry achieved between the aryl group and the carbonyl for −Y = −OCH₃ becomes responsible for a more effective transmission of the electronic effects of −Y closer to the reduction site, causing ρ to increase and the surface to curve down.

Conclusions

For all practical purposes, systems **1-X,Y** and **2-X,Y** have been selected at random, and thus our results exemplify the fact that nonlinear effects in Hammett-type free-energy relationships of electrochemical reactions should be rather common. Such effects can be explained on the basis of electronic and stereoelectronic considerations, but they may be either missed experimentally by choosing a narrow region of σ-values or become more pronounced by considering certain patterns of multiple substitution. Multiple substitution appears as a convenient means of tuning the redox potentials of redox systems useful as mediators (redox catalysts), sensors, or electrochromic materials. The fact that substitution effects are nonadditive introduces uncertainty in our a priori knowledge of the exact cumulative substitution effect. Nevertheless, if we were allowed to generalize from the data presented here, the emerging working hypothesis is that substituents operating by a purely inductive effect (e.g., both X and Y in benzyl viologens and X in the benzylpyridiniums) produce an about additive (linear) effect (as it could be illustrated by the effect of meta-substituted benzoyl group). On the other hand, substituents that can develop direct resonance interaction with a site undergoing electron transfer (e.g., Y in **2-X,Y**'s, which can interact through resonance with the carbonyl group) may introduce strong nonlinearity in the redox potential.[19] Further studies along these lines would involve the cumulative effect of three or more substituents, such as in the reduction of amines resulting from the reaction of **2-X,Y**'s and para-substituted anilines (Z).

References and Notes

(1) Isaacs, N. S. *Physical Organic Chemistry*, 2nd ed.; Longman Scientific and Technical: Essex, U.K., 1995; pp 164−165.

(2) See, for example: Um, I.-H.; Han, H.-J.; Ahn, J.-A.; Kang, S.; Buncel, E. *J. Org. Chem.* **2002**, *67*, 8475−8480.

(3) (a) Brown, H. C.; Okamoto, Y. *J. Am. Chem. Soc.* **1958**, *80*, 4979. (b) Yukawa, Y.; Tsuno, Y. *Bull. Chem. Soc. Jpn.* **1959**, *32*, 965−970. (c) Tsuno, Y.; Fujio, M. *Chem. Soc. Rev.* **1996**, *25*, 129−139.

(4) (a) Dubois, J.-E.; Ruasse, M.-F.; Argile, A. *J. Am. Chem. Soc.* **1984**, *106*, 4840−4845. (b) Argile, A.; Ruasse, M.-F. *J. Org. Chem.* **1983**, *48*, 209−214.

(5) (a) Fujio, M.; Rappoport, Z.; Uddin, M. K.; Kim, H.-J.; Tsuno, Y. *Bull. Chem. Soc. Jpn.* **2003**, *76*, 163−169. (b) Uddin, M. K.; Fujio, M.; Kim, H.-J.; Rappoport, Z.; Tsuno, Y. *Bull. Chem. Soc. Jpn.* **2002**, *75*, 1371−1379.

(6) O'Brien, M.; More O'Ferrall, R. A. *J. Chem. Soc., Perkin Trans.* **1978**, *2*, 1045.

(7) Leventis, N.; Zhang, G.; Rawashdeh, A.-M. M.; Sotiriou-Leventis, C. *Electrochim. Acta* **2003**, *48*, 2799−2806.

(8) Lever, A. B. P. *J. Porphyrins Phthalocyanines* **1999**, *3*, 488−499.

(9) Sauro, V. A.; Workentin, M. S. *J. Org. Chem.* **2001**, *66*, 831−838.

(10) Purely inductive effects and ρ-values less than unity are well-established for systems where the aryl group and the reacting site are separated by methylene spacers. For example, the ρ-values for the ionization in water of ArCO₂H, ArCH₂CO₂H, and ArCH₂CH₂CO₂H are 1.00, 0.56, and 0.24, respectively (see: Carey, F. A.; Sundberg, R. J. *Advanced Organic Chemistry, Part A: Structure and Mechanisms*, 3rd ed.; Plenum Press: New York, 1993; p 202.)

(11) (a) Leventis, N.; Rawashdeh, A.-M. M.; Zhang, G.; Elder, I. A.; Sotiriou-Leventis, C. *J. Org. Chem.* **2002**, *67*, 7501. (b) Leventis, N.; Elder, I. A.; Gao, X.; Bohannan, E. W.; Sotiriou-Leventis, C.; Rawashdeh, A.-M. M.; Overschmidt, K. R.; Gaston, K. R. *J. Phys. Chem. B* **2001**, *105*, 3663.

(12) Hale, P. D.; Boguslavsky, L. I.; Karan, H. I.; Lan, H. L.; Lee, H. S.; Okamoto, Y.; Skotheim, T. A. *Anal. Chim. Acta* **1991**, *248*, 155−161.

(13) (a) Kamogawa, H.; Suzuki, T. *Bull. Chem. Soc. Jpn.* **1987**, *60*, 794−796. (b) Miles, M. H.; Stilwell, D. E.; Hollins, R. A.; Henry, R. A. *Proc. Electrochem. Soc.* **1990**, *90*, 137−156. (c) Ashton, P. R.; Ballardini, R.; Balzani, V.; Belohradsky, M.; Gandolfi, M. T.; Philip, D.; Prodi, L.; Raymo, F. M.; Reddington, M. V.; Spencer, N.; Stoddart, J. F.; Venturi, M.; Williams, D. J. *J. Am. Chem. Soc.* **1996**, *118*, 4931−4951.

(14) Hansch, C.; Leo, A.; Taft, R. W. *Chem. Rev.* **1991**, *91*, 165.

(15) Meador, M. A. B.; Cubon, V. A.; Scheiman, D. A.; Bennett, W. R. *Chem. Mater.* **2003**, *15*, 3018−3025.

(16) Leventis, N.; Yang, J.; Fabrizio, E. F.; Rawashdeh, A.-M. M.; Oh, W. S.; Sotiriou-Leventis, C. *J. Am. Chem. Soc.* **2004**, *126*, 4094−4095.

(17) The substituent constant σ for the reduced NO₂ group has been previously reported to be −0.97.[7,11a,16] This value was obtained by linear extrapolation of a rather limited σ_{p-X}-range Hammett plot in order to accommodate only one species containing the NO₂•⁻ group (the 2e reduced form of 4-(p-NO₂-benzoyl)-N-methylpyridinium). Using $\sigma = -0.97$ in the response surface model of Figure 3B (both data sets with "block") yields a correlation coefficient, R^2, equal to 0.9750 and an RMS error equal to 0.01468. Since a total of 14 compounds (five containing the −NO₂•⁻ group) was used to fit the response surface model shown in Figure 3B, a refined value of σ was obtained. Thus, the largest R^2 values and the smallest RMS errors are achieved in this study by using a substituent constant of $\sigma = -0.62$ for NO₂⁻. Both regressions of $E_{1/2}(2)$ in Table 4 use this new σ value. At any rate, both numerical values for σ show that the 1e reduced −NO₂ group is one of the strongest electron donors.

(18) (a) Sjöström, M.; Wold, S. *Acta Chem. Scand. B* **1976**, *30*, 167−171. (b) Sjöström, M.; Wold, S. *Chem. Scr.* **1976**, *2*, 49−55. (c) Wold, S. *Chem. Scr.* **1974**, *5*, 97−106. (d) Wold, S.; Sjöström, M. *Chem. Scr.* **1972**, *2*, 49−55.

(19) We thank the reviewer who outlined this generalization.